JCTC Journal of Chemical Theory and Computation

pubs.acs.org/JCTC Article

Excited State-Specific CASSCF Theory for the Torsion of Ethylene

Sandra Saade and Hugh G. A. Burton*

Cite This: J. Chem. Theory Comput. 2024, 20, 5105−5114 Read Online

ABSTRACT: State-specific complete active space self-consistent field (SS-CASSCF) theory has emerged as a promising route to accurately predict electronically excited energy surfaces away from molecular equilibria. However, its accuracy and practicality for chemical systems of photochemical interest have yet to be fully determined. We investigate the performance of the SS-CASSCF theory for the low-lying ground and excited states in the double bond rotation of ethylene. We show that state-specific approximations with a minimal (2e,2o) active space provide comparable accuracy to state-averaged calculations with much larger active spaces, while optimizing the orbitals for each excited state significantly improves the spatial diffusivity of the wave function. However, the incorrect ordering of state-specific solutions causes excited state solutions to coalesce and disappear, creating unphysical discontinuities in the potential energy surface. Our findings highlight the theoretical challenges that must be overcome to realize practical applications of state-specific electronic structure theory for computational photochemistry.

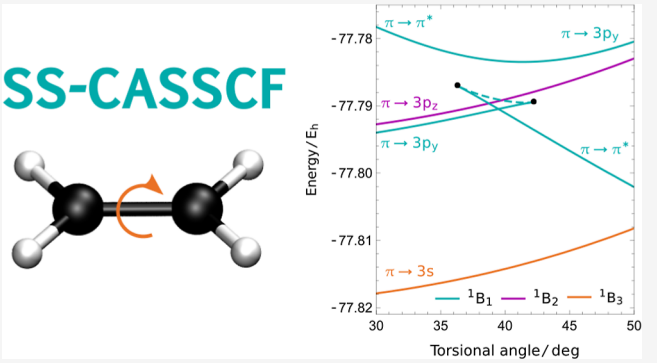

1. INTRODUCTION

Simulations of dynamic photochemical processes rely on faithful descriptions of ground- and excited-state energy surfaces away from molecular equilibria, but obtaining accurate and efficient predictions of electronic excitations remains a major challenge.[1] The prevalence of open-shell ground and excited states in photochemistry means that single-reference methods, such as equation-of-motion coupled cluster[2] and time-dependent density functional theory (TD-DFT),[3] are generally restricted to molecular structures around the equilibrium geometry. Therefore, computational studies rely on multiconfigurational methods, usually in the form of state-averaged (SA) complete active space self-consistent-field (CASSCF) theory.[4−6] However, state-averaging can give discontinuous energy surfaces due to "root-flipping" when electronic states cross.[7] Furthermore, large active spaces are required to capture all relevant states, and using a common set of orbitals does not account for bespoke orbital relaxation in charge transfer and Rydberg excitations.

Alternatively, recent research has explored the "state-specific (SS)" philosophy, where higher-energy electronic solutions are used to approximate individual excited states, which formally exist as saddle points on the exact electronic energy landscape.[8] The simplest approximation is self-consistent field (SCF) theory, where each excited state is represented by a single Slater determinant and the optimal orbitals are computed with either Hartree−Fock theory or Kohn−Sham density functional theory.[9−20] This approach has proved to be successful for predicting double excitations, charge transfer states,[9,12] and core excitations.[21] However, for open-shell states away from the ground state equilibrium geometry, one must resort to symmetry-broken SCF approximations that introduce spin or spatial symmetry contamination.[22,23] Furthermore, state-specific SCF solutions often disappear along a potential energy surface,[8,17,23−25] creating discontinuities that prevent dynamic simulations.

A more suitable state-specific approach for open-shell ground and excited states is multiconfigurational approximations, such as excited-state mean-field theory[26,27] or CASSCF theory.[28−32] Compared to state-averaging, these approaches provide bespoke orbitals for each excitation, meaning that smaller active spaces can be used.[32] Using a minimal multiconfigurational expansion to capture the key open-shell configurations is expected to alleviate the issues of disappearing SCF solutions. Previous work has shown that unphysical solutions can still arise if the wrong active space is chosen, and solutions can undergo symmetry breaking or disappear as the molecular structure changes.[32] However, the prevalence and significance of these irregularities for excited energy surfaces in larger molecules and basis sets of photochemical interest

Received: February 20, 2024
Revised: May 17, 2024
Accepted: May 22, 2024
Published: June 7, 2024

remain to be determined, preventing a firm evaluation of the long-term viability of SS-CASSCF theory.

In this contribution, we assess the performance of SS-CASSCF theory for the excited states in the double bond torsion of ethylene, which have been the subject of numerous theoretical and experimental studies over the past 50 years (see ref 33 for an excellent overview). The low-lying states of interest include the singlet and triplet $\pi \rightarrow 3s$ and $\pi \rightarrow 3p$ Rydberg excitations, the $\pi \rightarrow \pi^*$ single excitation (V), and the $(\pi)^2 \rightarrow (\pi^*)^2$ double excitation (Z). In particular, there has been significant debate about whether the $\pi \rightarrow \pi^*$ state has valence or Rydberg character,[33−44] which is compounded by the near degeneracy of the Rydberg and V single excitations and the nonvertical nature of the experimental excitation.[45−49] SA-CASSCF theory predicts the V state to be too diffuse in character,[38,43,44] as measured by the spatial second-order moment $\langle x^2 \rangle$, which is commonly attributed to the lack of dynamic correlation.[39−41] Furthermore, Angeli has highlighted the importance of dynamic σ-polarization and subsequent orbital contraction in the V state.[42]

At the planar D_{2h} structure, the bonding π and antibonding π^* orbitals transform as b_{3u} and b_{2g}, respectively, where the C−C bond coincides with the z-axis and the molecule lies in the yz-plane. The ground state and $\pi \rightarrow \pi^*$ open-shell singlet excitation correspond to the 1^1A_g and 1^1B_{1u} states. Following a photoexcitation to the 1^1B_{1u} state, the molecule is believed to rotate around the C−C bond toward the twisted D_{2d} structure, before a further pyramidalization of a $-CH_2$ group leads to a conical intersection with the ground state.[50−52] Accurate excited-state energies along this torsional mode are therefore essential, but SA-CASSCF is susceptible to root-flipping.[51] Since each state is dominated by at most two determinants, we expect a state-specific (2e, 2o) active space to give a qualitatively correct description.

In this work, we investigate the applicability of the SS-CASSCF (2,2) approach for the ground and excited states in the torsion of ethylene. We show that multiple ground state solutions can occur, and we identify suitable stationary points for the low-lying Rydberg excitations and the V and Z excited states. We find that SS-CASSCF (2,2) can provide comparable accuracy to SA-CASSCF calculations with much larger active spaces while avoiding the issues associated with state averaging such as root-flipping. On the other hand, we show that the incorrect ordering of excitations, potentially due to missing dynamic correlation or nondiffuse basis functions, can cause solutions to disappear, giving unphysical energy surfaces. Our findings highlight the promise and pitfalls of practical excited-state applications.

2. THEORY

2.1. SS CASSCF Theory. Electronic states with unpaired electrons are inherently multiconfigurational and must be modeled as a superposition of multiple Slater determinants using configuration interaction (CI). The CAS approach is the most common way to choose the subset of dominant configurations required to capture this "static" electron correlation. In CASCI, a subset of relevant active orbitals are chosen, and a CI expansion is built using every possible way of arranging the active electrons in these partially occupied orbitals. The remaining inactive and virtual orbitals are fully occupied, and empty, respectively, in each configuration.[4,53] As a truncated CI expansion, the CASCI wave function depends strongly on the choice of orbitals in the inactive, active, and virtual spaces. Therefore, the optimal wave function is usually identified by optimizing the orbital and CI coefficients self-consistently with the CASSCF approach.[4]

On each optimization step, the CASCI wave function is defined as

$$|\Psi_J\rangle = \sum_I |\Phi_I\rangle C_{IJ} \tag{1}$$

where C_{IJ} are the CI expansion coefficients for state J in terms of the active Slater determinants $|\Phi_I\rangle$. Variations in the CI and orbital coefficients can be represented using an exponential parametrization as

$$|\tilde{\Psi}_J\rangle = e^{\hat{R}} e^{\hat{S}} |\Psi_J\rangle \tag{2}$$

The anti-Hermitian operator $\hat{R}$ performs orbital rotations and is expressed in terms of the current orbitals[54−56]

$$\hat{R} = \sum_{p>q} R_{pq} \hat{E}^-_{pq} \tag{3}$$

where $\hat{E}^-_{pq} = \sum_{\sigma\in\uparrow,\downarrow} \hat{a}_{q\sigma}{}^\dagger \hat{a}_{p\sigma} - \hat{a}_{p\sigma}{}^\dagger \hat{a}_{q\sigma}$ is the anti-Hermitian singlet excitation operator.[57] Similarly, the $\hat{S}$ operator transforms the CI expansion by considering the transfer operators between the target state $|\Psi_J\rangle$ and the orthogonal states $|\Psi_K\rangle$ in the CASCI space as[56]

$$\hat{S} = \sum_{K\neq J} S_K (|\Psi_K\rangle\langle\Psi_J| - |\Psi_J\rangle\langle\Psi_K|) \tag{4}$$

The energy $E_J(\mathbf{R}, \mathbf{S}) = \langle\Psi_J| e^{-\hat{S}} e^{-\hat{R}} \hat{H} e^{\hat{R}} e^{\hat{S}} |\Psi_J\rangle$ is then a function of the variables S_K and R_{pq}, and the optimal CASSCF solutions are stationary points on the corresponding electronic energy landscape.

2.2. Computational Details. Since exact excited states are higher-index saddle points of the electronic energy landscape,[8] we expect SS-CASSCF excited states to also be saddle points of the energy. These can be identified using second-order optimization schemes, which also accelerate convergence if there is strong coupling between the orbital and CI degrees of freedom.[56,58−60] We employ the eigenvector-following technique[61] to target stationary points with a particular Hessian index, as described in ref 32. For open-shell single excitations, an initial guess can be prepared by first optimizing the orbitals for a suitable configuration state function (CSF) following the framework outlined in ref 57. Once an optimal SS-CASSCF solution has been found, it can be used as an initial guess for the next molecular geometry, allowing it to be tracked across the full potential energy surface. Since the Hessian index may change along a binding curve, the mode-controlled Newton−Raphson optimizer described in ref 32 is used to reconverge solutions at each geometry without prior knowledge of the Hessian index.

All calculations are performed using an in-house computational package developed in our group, which forms an extension to PYSCF.[62] We consider the aug-cc-pVDZ basis set,[63,64] which includes support for diffuse Rydberg states, and the smaller 6-31G basis set.[65] The convergence threshold is set to a root-mean-square gradient value of 10^{-7} E_h. SA- and SS-CASSCF(2,11) calculations were performed using the standard functionality in PYSCF.[62] Figures are plotted using

https://doi.org/10.1021/acs.jctc.4c00212
J. Chem. Theory Comput. 2024, 20, 5105−5114

Mathematica 12.0[66] and orbitals are visualized using the VMD software.[67]

3. RESULTS AND DISCUSSION

3.1. Summary of SS-CASSCF (2,2) Solutions. Using the aug-cc-pVDZ basis set, we first characterized the SS-CASSCF (2,2) solution space by starting from random MO and CI coefficients. We considered the planar D_{2h} geometry used in ref 68, which is provided in the Supporting Information. Low-energy solutions were targeted by searching for stationary points with Hessian indices between 0 and 10 using eigenvector-following. Up to 1000 random starting points were tested for each Hessian index. An extremely large number of low-energy solutions were identified, as illustrated in Figure 1, making a complete characterization of the solution space impossible.

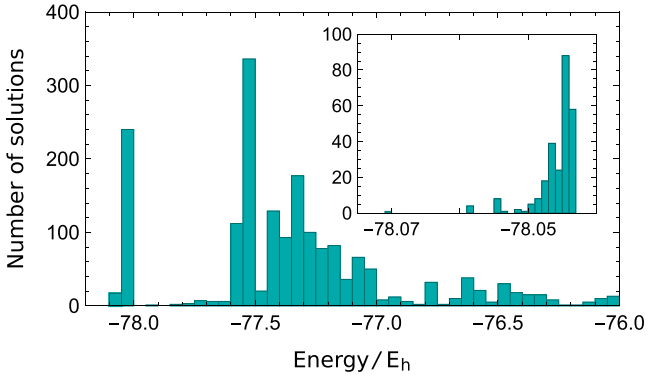

Figure 1. Number of SS-CASSCF (2,2) solutions identified at the D_{2h} geometry (aug-cc-pVDZ) using random starting guesses. Inset: The number of stationary points associated with the closed-shell ground state.

Instead, we focused our attention on the solutions corresponding to local minima, the low-energy singlet and triplet single excitations, and the Z double excitation. Starting from a preoptimized open-shell CSF allowed suitable stationary points to be found for the ($\pi \rightarrow 3s$), ($\pi \rightarrow 3p$), ($\pi \rightarrow \pi^*$) excitations, among others. The $(\pi)^2 \rightarrow (\pi^*)^2$ double excitation was identified by starting at the corresponding non-aufbau Slater determinant. Tracing the relevant solutions across the double bond rotation resulted in the ground- and excited-state energy surfaces shown in Figure 2.

Some solutions disappear along the torsional rotation. This disappearance can only occur if two stationary points coalesce on the CASSCF energy landscape at a pair annihilation point,[23,32] which mathematically corresponds to a fold catastrophe.[69] This coalescence is associated with the onset of a zero eigenvalue in the Hessian matrix of second derivatives with respect to the wave function parameters, and similar phenomena occur for multiple Hartree−Fock solutions.[18,23,32,70] The other solution involved in the pair annihilation can be identified using a line search in the direction of the eigenvector corresponding to the zero Hessian eigenvalue, as detailed in Appendix A.

In the following sections, we characterize the local minima (Section 3.2) and the valence and Rydberg excitations (Section 3.3). Finally, we highlight how the SS-CASSCF solutions change if we use a smaller basis set that cannot describe Rydberg states (Section 3.4).

3.2. Multiple Local Minima. Although there is only one minimum on the exact energy landscape,[8] the SS-CASSCF (2,2) approximation yields five minima at the planar structure, corresponding to a unique global minimum and a 4-fold degenerate set of local minima. The partially occupied natural orbitals for these solutions reveal that the global minimum corresponds to the expected $\{\pi, \pi^*\}$ active orbitals with occupations of 1.9150 and 0.0850, respectively (Figure 3A). In contrast, the active orbitals for the local minima break the spatial symmetry and correspond to the quasi-localized C−H σ and σ^* orbitals, with the 4-fold degeneracy arising from the four C−H bonds (Figure 3B). Since the true ground state is dominated by one closed-shell configuration, both active spaces include one orbital that is almost doubly occupied and one that is almost unoccupied. The active orbital with $n_{occ} \approx 2$ can be swapped for a doubly occupied inactive orbital without significantly changing the energy, leading to multiple

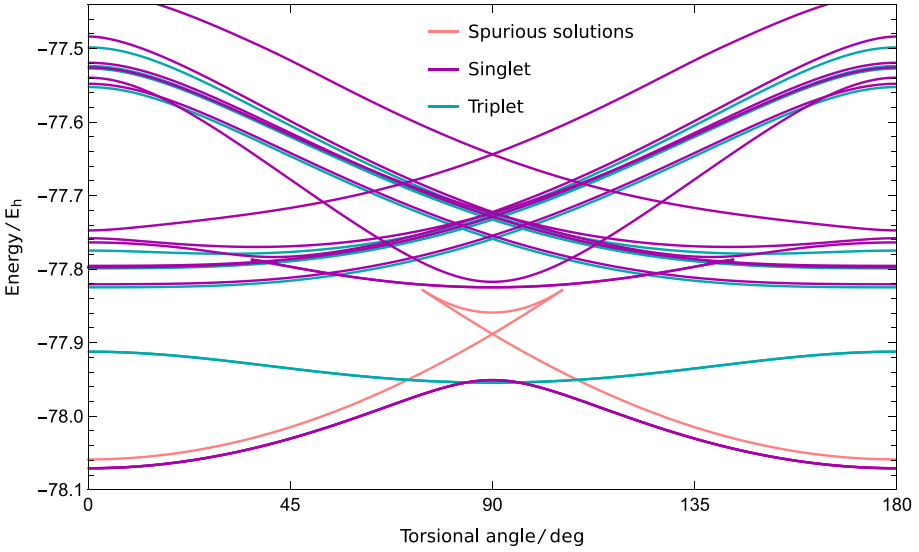

Figure 2. Summary of the physically meaningful singlet and triplet SS-CASSCF (2,2) solutions in ethylene (aug-cc-pVDZ) as well as the spurious local minima and index-1 saddle point (see Figure 3C).

https://doi.org/10.1021/acs.jctc.4c00212
J. Chem. Theory Comput. 2024, 20, 5105−5114

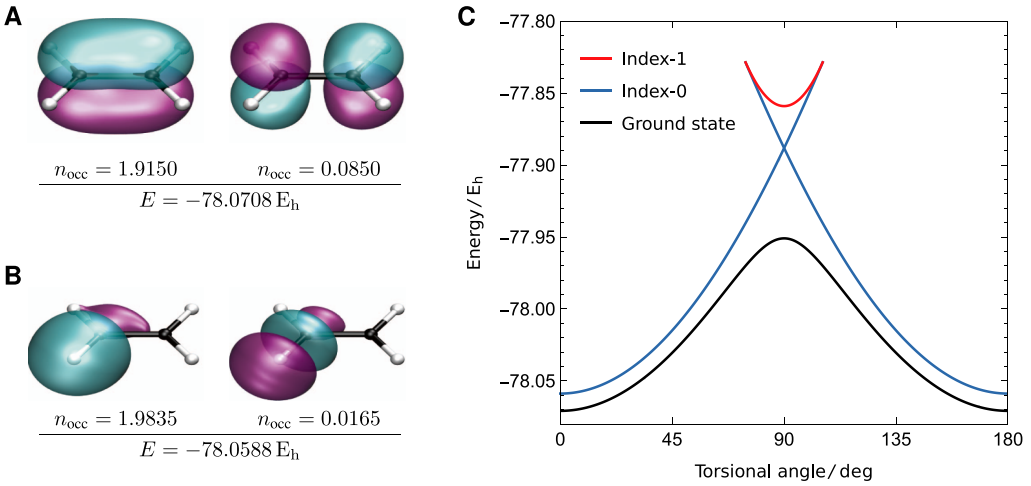

Figure 3. Comparison of the natural active orbitals for the SS-CASSCF (2,2) minima at the planar geometry (aug-cc-pVDZ). The global minimum (A) gives a smooth torsional barrier, while the local minima (B) give a cusp at 90° and disappear in a pair annihilation point at 106°.

Table 1. Vertical Excitation Energies (eV) Computed with SS- and SA-CASSCF Are Compared against Literature Values and TBE[d]

state		SS-(2,2)[a]	SS-(2,11)[a]	SA(5/4)-(2,11)[a]	SA(sym)-(2,11)[a]	ex-FCI[b]	TBE[c]
1^1A_g		0.00	0.00	0.00	0.00	0.00	0.00
1^1B_{1u}	$\pi \rightarrow \pi^*$	8.36	8.38	8.06	8.47	7.93	8.00
1^1B_{3u}	$\pi \rightarrow 3s$	6.81	6.89	6.48	6.92	7.31	7.45
1^1B_{1g}	$\pi \rightarrow 3p_y$	7.44	7.57	7.12	7.57	8.00	8.06
1^1B_{2g}	$\pi \rightarrow 3p_z$	7.49	7.58	7.14	7.58	8.00	8.11
1^3B_{1u}	$\pi \rightarrow \pi^*$	4.32	4.46	4.33	4.63	4.55	4.55
1^3B_{3u}	$\pi \rightarrow 3s$	6.70	6.80	6.35	6.84	7.16	7.29
1^3B_{1g}	$\pi \rightarrow 3p_y$	7.40	7.54	7.08	7.54	7.93	8.02
1^3B_{2g}	$\pi \rightarrow 3p_z$	7.43	7.54	7.09	7.54	7.93	8.04
MSE	Rydberg	−0.51	−0.40	−0.85	−0.39	0.00	
	valence	0.10	0.18	−0.05	0.31	0.00	
MUE	Rydberg	0.51	0.40	0.85	0.39	0.00	
	valence	0.33	0.27	0.17	0.31	0.00	

[a]This work (aug-cc-pVDZ). [b]Reference 68 (aug-cc-pVDZ). [c]Reference 33 (approximately CBS). [d]Errors are provided relative to the ex-FCI values with the same basis set (aug-cc-pVDZ) and geometry, taken from ref 68. Two different state-averaging protocols are considered, as described in the main text.

representations of the ground state, as described in ref 32. Therefore, in the absence of strong static correlation at the D_{2h} geometry, the different minima attempt to capture dynamic correlation in either the C−H σ or C−C π bonds.

Although both sets of minima provide a reasonable approximation to the planar geometry, choosing the right active orbitals is essential for computing physically meaningful energy surfaces.[32] The global minimum can be followed across the full torsion to give a smooth rotational barrier (Figure 3C) because the $\{\pi, \pi^*\}$ active orbitals can correctly break the C−C π bond. In contrast, the energy of the C−H $\{\sigma, \sigma^*\}$ local minimum does not reach a maximum at 90°, and the solution eventually coalesces with an index-1 saddle point, both of which disappear in a pair annihilation point at 106°. The corresponding index-1 saddle point can be traced from 106 back to 74°, where it coalesces with a symmetry-related C−H $\{\sigma, \sigma^*\}$ local minimum that can be identified at the 180° planar structure. This coalescence pattern between symmetry-related local minima and a connecting index-1 saddle point is a common feature of nonlinear wave function approximations.[23,32,70] Its presence for the local SS-CASSCF (2,2) minima in ethylene re-emphasizes the importance of selecting meaningful active spaces that can faithfully capture the static correlation across a particular chemical reaction coordinate.

3.3. Valence and Rydberg Excitations. The low-lying singly excited states in ethylene correspond to excitations from the π orbital to a 3s or 3p Rydberg orbital and the valence $\pi \rightarrow \pi^*$ excitation. A SS-CASSCF (2,2) solution for each of the corresponding singlet and triplet excitations can be identified at the planar geometry. The orbital assignment and excitation energies are tabulated in Table 1, alongside literature benchmark values computed with extrapolated FCI[68] (ex-FCI). In addition, we run a SS-CASSCF (2,11) calculation for the lowest-energy state of each symmetry to assess the effect of the active space size on the excited-state energy prediction. We compare against two SA-CASSCF (2,11) procedures using the same basis set and geometry. The first approach, denoted SA(5/4)-(2,11), performs a state-averaged optimization over all five tabulated singlet states or four triplet states with individual calculations for each spin sector. The second method, denoted SA(sym)-(2,11), follows the state averaging protocol outlined in ref 38, whereby individual calculations are performed for excited states of each irreducible representation, including the $\pi \rightarrow$ d Rydberg states, and the ground state is

https://doi.org/10.1021/acs.jctc.4c00212
J. Chem. Theory Comput. 2024, 20, 5105−5114

Table 2. Comparison of the Second-Order Moment $\langle x^2 \rangle$ (a_0^2) and Oscillator Strength f(au) for SS- and SA-CASSCF at the Planar D_{2h} Geometry[c]

		SS-(2,2)[a]		SS-(2,11)[a]		SA(5/4)-(2,11)[a]		SA(sym)-(2,11)[a]		TBE[b]	
state		$\langle x^2 \rangle$	f	$\langle x^2 \rangle$	f	$\langle x^2 \rangle$	f	$\langle x^2 \rangle$	f	$\langle x^2 \rangle$	f
1^1A_g		11.68		11.74		12.00		11.74		11.78	
1^1B_{1u}	$\pi \rightarrow \pi^*$	22.52	0.298	21.29	0.356	22.45	0.364	21.66	0.355	17 ± 1	0.333
1^1B_{3u}	$\pi \rightarrow 3s$	21.55	0.066	21.03	0.071	21.31	0.103	21.13	0.072	23.96	0.069
1^1B_{1g}	$\pi \rightarrow 3p_y$	17.89		17.64		17.59		17.64		20.38	
1^1B_{2g}	$\pi \rightarrow 3p_z$	18.84		18.43		18.36		18.43		21.53	
1^3B_{1u}	$\pi \rightarrow \pi^*$	11.74		11.77		12.14		11.94		11.69	
1^3B_{3u}	$\pi \rightarrow 3s$	21.40		21.07		20.97		21.24		23.45	
1^3B_{1g}	$\pi \rightarrow 3p_y$	17.68		17.46		17.40		17.46		19.66	
1^3B_{2g}	$\pi \rightarrow 3p_z$	18.48		18.16		18.13		18.16		20.35	
MSE	Rydberg	−2.25		−2.59		−2.60		−2.55			
	valence	1.82		1.44		2.04		1.62			
MUE	Rydberg	2.25		2.59		2.60		2.55			
	valence	1.89		1.47		2.04		1.65			

[a]This work (aug-cc-pVDZ). [b]Reference 33 (approximately CBS). [c]Errors are provided relative to the TBE values taken from ref 33. Two different state-averaging protocols are considered, as described in the main text.

optimized separately. In this setup, the B_{3u}, B_{1g}, and B_{2g} excitations tabulated in Table 1 correspond to state-specific calculations. For reference, we also include the theoretical best estimate (TBE) from ref 33.

Compared to the ex-FCI values from ref 68, both the SS-CASSCF (2,2) and the SS-CASSCF (2,11) Rydberg excitation energies are consistently underestimated by around 0.5 eV, as shown by the mean signed error (MSE) in Table 1. The larger (2,11) active space only improves the accuracy by around 0.1 eV compared to SS-CASSCF (2,2). Since the SS-CASSCF approximation predominantly captures static electron correlation, this consistent shift suggests that there is an imbalance between the dynamic correlation in the ground and Rydberg states, supporting the findings of ref 38. In particular, the spatially compact nature of the ground state leads to regions of higher electron density and thus greater dynamic correlation than the more diffuse Rydberg states. Therefore, both SS-CASSCF (2,2) and (2,11) underestimate the ground-state energy and, by extension, the Rydberg excitation energies. In comparison, SA-CASSCF (5/4)-(2,11) provides a less accurate excitation energy than either of the SS approaches, which is expected due to the lack of specific orbital relaxation for the individual Rydberg states. The fact that the valence $\pi \rightarrow \pi^*$ excitation is better approximated by using SA(5/4)-(2,11) is likely to be the result of error cancellation.

Compared to the −0.5 eV underestimate for the Rydberg excitation energies, the SS-CASSCF (2,2) approximation overestimates the V excitation energy by 0.43 eV. This overestimate can be understood because the $\pi \rightarrow \pi^*$ excited state is dominated by zwitterionic resonance structures with a larger dynamic correlation energy than the ground state, which is not captured by the CASSCF approximation.[39,40,42] This excitation energy is essentially unchanged using the much larger SS-CASSCF (2,11) active space. On the other hand, the SA(sym)-(2,11) approach provides a much greater overestimate of 0.54 eV for the valence $\pi \rightarrow \pi^*$ excitation energy since the orbitals are optimized for a SA density that also includes the $\pi \rightarrow d_{xz}$ Rydberg state. Therefore, the SS protocols both provide comparable accuracy to the SA(sym)-(2,11) excitation energies, while avoiding the issues associated with SA optimization.

The quality of the wave function, and the degree of Rydberg character, can also be measured through the $\langle x^2 \rangle$ value, which can vary significantly for a small change in energy.[41] Compared to the TBEs taken from ref 33, the SS-CASSCF (2,2) approach provides estimates of $\langle x^2 \rangle$ with a MUE of 2.25 a_0^2 and 1.89 a_0^2 for the Rydberg and valence states (including the ground state), respectively (Table 2). Surprisingly, the SS-CASSCF (2,11) improves the second-order moment of the valence excited states but worsens the description of the Rydberg excitations. The largest errors are obtained with the SA(5/4)-(2,11) procedure, demonstrating the advantage of using a SS approach to optimize the orbitals for each state individually.

Whether the 1^1B_{1u} $\pi \rightarrow \pi^*$ state has predominant valence or Rydberg character has long been disputed due to the challenge of reproducing the experimental band absorption maximum at 7.6 eV. Recent studies have confirmed that nonadiabatic effects[36,47,48] shift this experimental value away from the vertical excitation energy that is closer to 8.0 eV,[33,49,68] while dynamic correlation and σ-polarization are expected to cause the excited state π^* orbital to contract.[42] This spatial contraction is not easily seen in SA-CASSCF,[42−44] and previous SA-CASSCF (2,11) calculations with an ANO basis set reported a large $\langle x^2 \rangle$ value of 44.1 a_0^2.[38] In contrast, our SS- and SA-CASSCF calculations using the aug-cc-pVDZ basis set all provide estimates between $\langle x^2 \rangle$ = 21.29 a_0^2 and 22.52 a_0^2, which is much closer to the TBE (Table 2), while the SS-CASSCF (2,2) excited state visually yields a more contracted π^* orbital (Figure 4) compared to the ground state solution (Figure 3A).

The relatively accurate spatial diffusivity of the SS wave functions is also reflected in the oscillator strength for $\pi \rightarrow \pi^*$ excitation. Since the ground and excited states are represented with different sets of orbitals, we use the extended non-orthogonal Wick's theorem[71,72] implemented in the LIBGNME software package[73] to evaluate the transition dipole moment. The SS-CASSCF (2,2) and (2,11) approaches predict the oscillator strength with deviations of −0.035 and 0.023 au from the TBE, respectively (Table 2). This accuracy suggests that the SS approach minimizes contamination from nearby Rydberg states, which have a weaker oscillator strength

https://doi.org/10.1021/acs.jctc.4c00212
J. Chem. Theory Comput. 2024, 20, 5105−5114

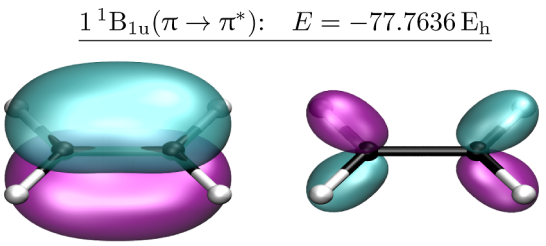

Figure 4. HOMO and LUMO orbitals for the 1^1B_{1u} ($\pi \rightarrow \pi^*$) excitation in planar ethylene. The π^* orbital is significantly contracted compared to Figure 3A.

than the valence excitation. The $\pi \rightarrow 3s$ oscillator strengths are even more accurate, with deviations of −0.003 and 0.002 au for the SS-(2,2) and (2,11) approaches, respectively. By comparison, the SA(5/4)-(2,11) calculation overestimates both values by around 0.030 au.

Compared to the ex-FCI[68] and TBE[33] results, the SS-CASSCF (2,2) and (2,11) approximations both erroneously predict that the valence 1^1B_{1u} state is higher in energy than the Rydberg 1^1B_{1g} and 1^1B_{2g} states at the planar geometry. This incorrect ordering has a subsequent effect on the corresponding excited-state energy surfaces along the torsional rotation. As the molecule twists away from the planar geometry, the spatial point group changes from D_{2h} to D_{2d}. Under this decrease in symmetry, the planar 1^1B_{1u} and 1^1B_{1g} states both transform as the same $^1B_1$ irreducible representation, meaning that they can couple through the Hamiltonian. The $\pi \rightarrow \pi^*$ and $\pi \rightarrow 3p_y$ excited states become lower and higher in energy, respectively, eventually leading to an avoided crossing (cyan in Figure 5). We characterize this avoided crossing as unphysical since it is not consistent with the ordering of the 1^1B_{1u} and 1^1B_{1g} states observed in high-accuracy results.[33,68]

SS approximations are known to have unphysical solutions or coalescence points in the vicinity of avoided crossings.[17,23,32] Here, we see that the higher energy solution, corresponding to the planar $\pi \rightarrow \pi^*$ state, evolves continuously into the $\pi \rightarrow 3p_y$ state at the avoided crossing, as shown in Figure 5. In contrast, the lower energy solution continues to increase in energy until it eventually disappears in a pairwise coalescence point at 42°. The other solution involved in the coalescence can be followed back to 37°, where it coalesces with a third solution that corresponds to the $\pi \rightarrow \pi^*$ state after the avoided crossing. These two solutions, which together form the lower part of the avoided crossing, have an unphysical state intersection around 39°. Therefore, the lower $\pi \rightarrow 3p_y$ solution is the only physically meaningful state that cannot be followed across the full torsional rotation, creating potential issues for the use of SS-CASSCF theory in ab initio excited-state molecular dynamics. We unsuccessfully attempted to avoid this issue using a (2e, 3o) active space that contained both the π^* and $3p_y$. Furthermore, the same disappearance also occurs for the SS-CASSCF (2,11) solutions tabulated in Table 1, while the large number of zero Hessian eigenvalues with this active space prevents a straightforward analysis of the complementary solutions using the method described in Appendix A. On the other hand, the SS philosophy successfully avoids the more widespread discontinuities that occur in SA calculations, as seen in Figure 6 of ref 51.

Finally, we consider the double excitation $(\pi)^2 \rightarrow (\pi^*)^2$, which cannot be captured by linear response formalisms such as TD-DFT. Starting from the non-aufbau Slater determinant

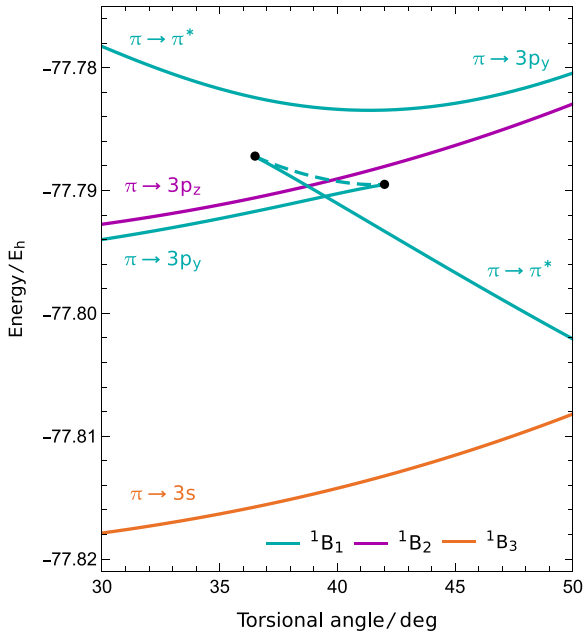

Figure 5. SS-CASSCF (2,2) predicts the wrong ordering for the $\pi \rightarrow \pi^*$ and $\pi \rightarrow 3p_y$ states at the planar geometry, leading to an avoided crossing along the torsional rotation. The lower energy solution disappears at a pair annihilation point (42°) and a new discontinuous SS-CASSCF (2,2) solution emerges (37°), which represents the $\pi \rightarrow \pi^*$ state at larger torsional angles. Rydberg states with different symmetries are unaffected.

at the planar geometry, the corresponding SS-CASSCF (2,2) solution can be identified with an excitation energy of ΔE = 14.46 eV and provides a continuous energy surface across the full torsional rotation (Figure 2). This state is less well covered in the literature, but benchmark values from the QUEST data set[74,75] and ref 52 predict an excitation energy closer to 13−13.6 eV. Therefore, the SS-CASSCF (2,2) overestimates the double excitation energy, which we believe is due to the unbalanced dynamic correlation between the ground and zwitterionic excited states, as already seen for the $\pi \rightarrow \pi^*$ excitation.

3.4. Consequences of a Nondiffuse Basis Set.

The presence of low-energy Rydberg states means that diffuse basis functions are considered to be essential for accurately predicting the excited states in ethylene.[33,35,37] We also performed SS-CASSCF (2,2) calculations using the 6-31G basis set, highlighting how the lack of diffuse basis functions can fundamentally change the pattern of SS solutions in ethylene. While the ground state exhibited a global minimum and 4-fold degenerate local minima that are directly analogous to the aug-cc-pVDZ basis, we were unable to find any physically meaningful approximations to the singly excited $\pi \rightarrow \pi^*$ or the doubly excited $(\pi)^2 \rightarrow (\pi^*)^2$ energy surfaces.

To target the $\pi \rightarrow \pi^*$ excited state, we started the SS-CASSCF (2,2) optimization from the output of a SA-CASSCF (2,2) calculation at the planar geometry. The planar molecular structure was identified through a geometry optimization using the B3LYP functional and is provided in the Supporting Information. Starting from the SA $\pi \rightarrow \pi^*$ initial guess gave a stationary point with symmetry-pure orbitals, with the natural orbitals corresponding to the localized zwitterionic configurations (Figure 6A). However, this solution only exists up to a torsional angle of 0.02°, where it disappears in a pair

https://doi.org/10.1021/acs.jctc.4c00212
J. Chem. Theory Comput. 2024, 20, 5105−5114

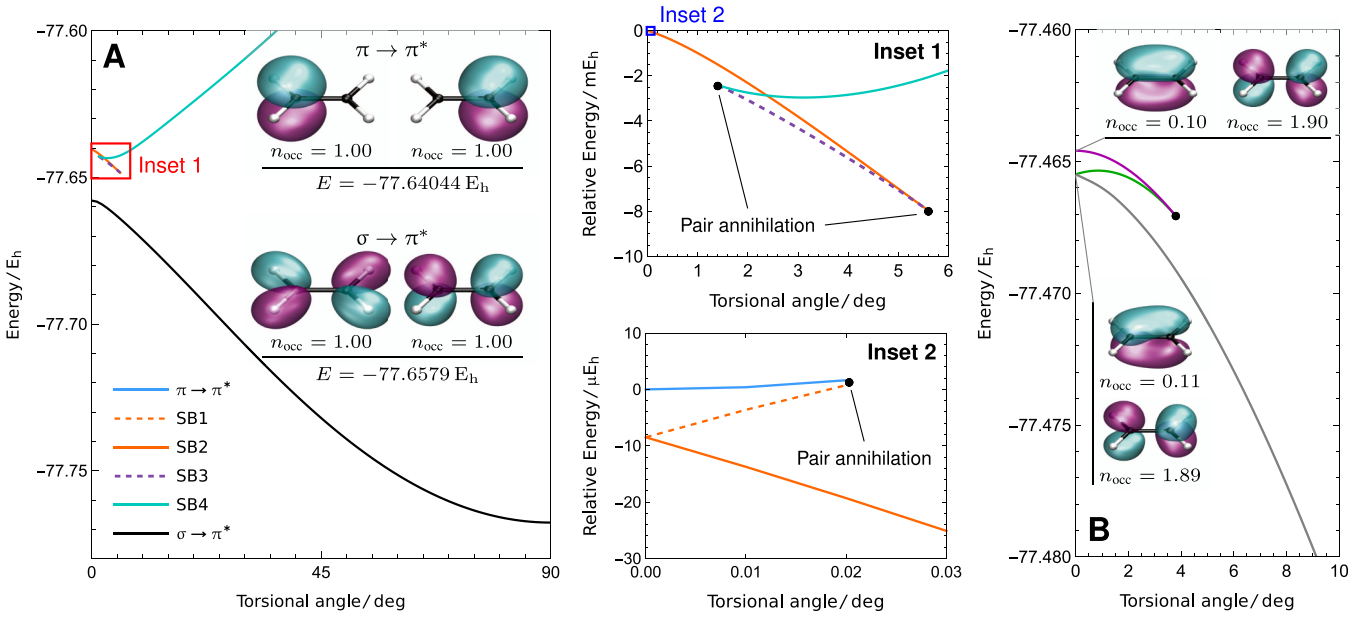

Figure 6. SS-CASSCF (2,2) with the 6-31G basis set does not provide physically meaningful energy surfaces for the singly excited $\pi \rightarrow \pi^*$ state or the doubly excited $(\pi)^2 \rightarrow (\pi^*)^2$ state. (A) This approximation predicts the wrong ordering of the $\pi \rightarrow \pi^*$ and $\sigma \rightarrow \pi^*$ states at the planar geometry, leading to a series of symmetry-broken (SB) solutions and an unphysical avoided crossing. (B) The symmetry-pure solution (purple) corresponding to the $(\pi)^2 \rightarrow (\pi^*)^2$ excitation disappears at a torsional angle of 3.8°, giving an unphysical potential energy surface.

annihilation point (Figure 6: inset 2). A complex pattern of coalescing solutions can be found that ultimately connects the $\pi \rightarrow \pi^*$ solution to another solution that emerges at 1.5°, which increases in energy for higher torsional angles (cyan in Figure 6A).

Alternatively, searching for the $\pi \rightarrow \pi^*$ state at 90° yields a solution that exists all the way to 0° (black in Figure 6). However, the corresponding natural orbitals at the planar geometry indicate that this solution evolves into the $^1B_{1g}$ $\sigma \rightarrow \pi^*$ excitation, which is known to be higher in energy than the $\pi \rightarrow \pi^*$ state using high-accuracy methods.[33] Ultimately, the smaller 6-31G basis set results in the incorrect ordering of the $^1B_{1g}$ and $^1B_{1u}$ excited states because it cannot describe the diffuse character of the $\pi \rightarrow \pi^*$ state, as indicated by the small $\langle x^2 \rangle$ value of 12.24 a_0^2. Like the interaction between the $\pi \rightarrow \pi^*$ excitation and the Rydberg states using the aug-cc-pVDZ basis, this ordering problem creates an unphysical avoided crossing that causes SS-CASSCF (2,2) solutions to coalesce and disappear as the double bond rotates, leading to catastrophic potential energy surfaces. This avoided crossing corresponds to the cyan (labeled SB4) and black curves in Figure 6A, where the cyan, orange, and dashed purple curves in Inset 1 form the upper branch with the typical structure seen elsewhere.[23,32] The $\sigma \rightarrow \pi^*$ (black) state evolves continuously into the $\pi \rightarrow \pi^*$ state after the avoided crossing, while the symmetry-broken SB4 solution disappears at 1.5° in a series of pair annihilation points that eventually lead to the symmetry-pure $\pi \rightarrow \pi^*$ (blue) state.

Similarly, starting from the SA states allows a symmetry-pure SS-CASSCF (2,2) solution to be identified for the $(\pi)^2 \rightarrow (\pi^*)^2$ double excitation (solid purple in Figure 6B). However, this solution also disappears as the molecule is twisted and cannot be traced beyond 3.8°, where it coalesces with another solution (green in Figure 6B). This second state can be traced back to the planar geometry, where it forms a pair of degenerate solutions with natural orbitals that break the spatial symmetry (the degeneracy is lifted for nonzero torsional angles). The other degenerate solution can be followed across the full torsional mode for angles between 0 and 180° (gray in Figure 6B). However, as these degenerate solutions break the spatial symmetry and cross in energy at 0°, neither predicts a stationary point in the excited energy surface at the planar geometry. Consequently, the SS-CASSCF (2,2) approximation is not able to provide any meaningful potential energy surface for the $(\pi)^2 \rightarrow (\pi^*)^2$ Z state of ethylene using the 6-31G basis, and it is vital that the basis set is sufficient for the excited states of interest.

4. CONCLUDING REMARKS

Excited SS-CASSCF approximations promise to overcome the challenges of SA-CASSCF theory for predicting excited energy surfaces by facilitating calculations with smaller active spaces and avoiding root-flipping discontinuities. In this work, we assessed the performance of the SS-CASSCF (2,2) approach for the valence and Rydberg excitations in the torsion of ethylene using the aug-cc-pVDZ and 6-31G basis sets. While a large number of SS-CASSCF (2,2) solutions exist, we were able to target physically meaningful stationary points for the low-lying excited states at the planar D_{2h} structure using the aug-cc-pVDZ basis set. These solutions provided excitation energies and properties for ethylene that are comparable to those of much larger SA and SS approximations. Furthermore, most of the SS-CASSCF (2,2) solutions using aug-cc-pVDZ can be continuously followed across the torsional rotation, avoiding the root-flipping problems in SA-CASSCF and the limitations of single-reference linear-response methods.

While we have only considered the excited states of ethylene, our findings support previous work[32] showing that SS-CASSCF can be applied with only the active orbitals required for the open-shell character of each excitation. In ethylene, a (2,2) active space is sufficient to describe the torsional rotation, single excitations, and the doubly

https://doi.org/10.1021/acs.jctc.4c00212
J. Chem. Theory Comput. 2024, 20, 5105−5114

$(\pi)^2 \rightarrow (\pi^*)^2$ excited state. However, larger molecules with more complex excitations or broken chemical bonds may require larger active spaces, and this must be determined on a case-by-case basis. Regardless, the findings of this work, and others,[29,32] support the view that the SS philosophy can successfully avoid many of the issues associated with SA calculations, such as root-flipping and the large active spaces required to simultaneously predict many excitations.

The apparent imbalance between the missing dynamic correlation in Rydberg and valence excited states means that SS-CASSCF (2,2) and (2,11) fail to provide the correct state ordering in planar ethylene. This incorrect ordering of the $\pi \rightarrow 3p_y$ and $\pi \rightarrow \pi^*$ states using the aug-cc-pVDZ basis set creates an artificial avoided crossing away from the planar geometry that manifests as a pair annihilation point, where one of the states coalesces with another unphysical solution and disappears. Therefore, there is a trade-off between coalescing solutions and root-flipping discontinuities in SS- and SA-CASSCF, respectively. Since the reference SS-CASSCF (2,2) solution mathematically disappears, these irregularities cannot be remedied by post-CASSCF correlation methods such as CASPT2,[76−78] multireference CI,[79] or even multistate CASPT2.[80] Instead, we believe that a SS wave function approximation optimized in the presence of dynamic correlation will be required to stop states from disappearing. One possibility is to use a larger active space, as we tried in this work. However, larger active spaces are associated with many additional distinct CASSCF solutions if there are active orbitals with occupation numbers close to 0 or 2, making it much harder to identify a well-defined and consistent solution for each excitation. Furthermore, for the ethylene $\pi \rightarrow \pi^*$ excited state, the dynamic correlation is associated with σ-polarization,[42] which requires a full-valence active space to account for the relaxation within the σ-framework.

Finally, SS-CASSCF(2,2) calculations with the 6-31G basis set cannot capture the diffuse character of the $\pi \rightarrow \pi^*$ state at all, which is predicted to be too high in energy. This error causes an artificial avoided crossing with the $\sigma \rightarrow \pi^*$ excitation, and we were unable to find any meaningful energy surfaces for the $\pi \rightarrow \pi^*$ or $(\pi)^2 \rightarrow (\pi^*)^2$ states. These observations emphasize the importance of using sufficient basis sets for the excited states of interest and also highlight the danger of assessing SS approximations using inadequate basis sets.

Ultimately, the coalescence and disappearance of solutions remain the primary obstacle to practical excited SS calculations. These coalescence points are mainly due to the unbalanced description of different states, such as valence and Rydberg excitations. While this imbalance might be due to the lack of dynamic correlation, an alternative perspective is that the SS-CASSCF approximation simply is not the right reference for molecular excited states. Since the ethylene single excitations correspond to open-shell singlets, further restricting the wave function to a single CSF would not change our results. Instead, we believe that new wave function approximations, which explicitly include the effects of dynamic σ-polarization and orbital contraction in excited states, may provide more accurate and efficient energy surfaces for photochemistry, and we intend to pursue this direction in future work.

APPENDIX A: LINE SEARCH AT PAIR ANNIHILATION POINTS

The disappearance of a SS-CASSCF solution as the molecular structure changes indicates the existence of a pair annihilation point, which mathematically corresponds to the coalescence of two stationary points in a fold catastrophe.[69] The Hessian index of the two solutions must differ by at most one downhill direction. For example, an index-1 saddle point can coalesce with a minimum or an index-2 saddle point. At the coalescence point itself, the two solutions become identical and one of the Hessian eigenvalues becomes zero. To find the other solution involved in this pair annihilation, we exploit the fact that the eigendirection corresponding to the zero Hessian eigenvalue points from one solution to the other if we are close enough to the coalescence point. We can then identify constrained stationary points of the energy using a line search along this eigendirection and use the one that is closest to the original solution as an initial guess for a SS-CASSCF calculation. This subsequent SS-CASSCF state will converge to the complementary solution involved in the pair annihilation. Through this procedure, we can fully map the pattern of coalescing solutions in SS-CASSCF theory.

ASSOCIATED CONTENT

Supporting Information

The Supporting Information is available free of charge at https://pubs.acs.org/doi/10.1021/acs.jctc.4c00212.

Planar ethylene structure (a_0) used for aug-cc-pVDZ calculations (XYZ)

Planar ethylene structure (a_0) used for 6-31G calculations (XYZ)

AUTHOR INFORMATION

Corresponding Author

Hugh G. A. Burton − *Yusuf Hamied Department of Chemistry, University of Cambridge, Cambridge CB2 1EW, U.K.*; orcid.org/0000-0002-1342-2056; Email: hgaburton@gmail.com

Author

Sandra Saade − *Yusuf Hamied Department of Chemistry, University of Cambridge, Cambridge CB2 1EW, U.K.; Department of Chemistry, Physical and Theoretical Chemical Laboratory, University of Oxford, Oxford OX1 3QZ, U.K.*; Present Address: Laboratory of Computational Science and Modeling, Institut des Matériaux, École Polytechnique Fédérale de Lausanne, 1015 Lausanne, Switzerland; orcid.org/0009-0008-6163-0758

Complete contact information is available at: https://pubs.acs.org/10.1021/acs.jctc.4c00212

Notes

The authors declare no competing financial interest.

ACKNOWLEDGMENTS

H.G.A.B. gratefully acknowledges funding from New College, Oxford (Astor Junior Research Fellowship) and Downing College, Cambridge (Kim and Julianna Silverman Research Fellowship). The authors thank Nicholas Lee, David Tew, and Pierre-François Loos for discussions and research support.

REFERENCES

(1) González, L.; Escudero, D.; Serrano-Andrés, L. Progress and Challenges in the Calculation of Electronic Excited States. *ChemPhysChem* **2012**, *13*, 28−51.
(2) Bartlett, R. J. Coupled-cluster theory and its equation-of-motion extensions. *Wiley Interdiscip. Rev.: Comput. Mol. Sci.* **2012**, *2*, 126−138.
(3) Dreuw, A.; Head-Gordon, M. Single-Reference ab Initio Methods for the Calculation of Excited States of Large Molecules. *Chem. Rev.* **2005**, *105*, 4009−4037.
(4) Roos, B. O.; Taylor, P. R.; Sigbahn, P. E. M. A complete active space SCF method (CASSCF) using a density matrix formulated super-CI approach. *Chem. Phys.* **1980**, *48*, 157−173.
(5) Roos, B. O.; Lindh, R.; Malmqvist, P. Å.; Veryazov, V.; Windmark, P.-O. *Multiconfigurational Quantum Chemistry*; Wiley, 2016.
(6) Werner, H.-J.; Meyer, W. A quadratically convergent MCSCF method for the simultaneous optimization of several states. *J. Chem. Phys.* **1981**, *74*, 5794−5801.
(7) Zaitsevskii, A.; Malrieu, J.-P. The discontinuities of state-average MCSCF potential surfaces. *Chem. Phys. Lett.* **1994**, *228*, 458−462.
(8) Burton, H. G. A. Energy Landscape of State-Specific Electronic Structure Theory. *J. Chem. Theory Comput.* **2022**, *18*, 1512−1526.
(9) Gilbert, A. T. B.; Besley, N. A.; Gill, P. M. W. Self-Consistent Field Calculations of Excited States Using the Maximum Overlap Method (MOM). *J. Phys. Chem. A* **2008**, *112*, 13164−13171.
(10) Besley, N. A.; Gilbert, A. T. B.; Gill, P. M. W. Self-consistent-field calculations of core excited states. *J. Chem. Phys.* **2009**, *130*, 124308.
(11) Barca, G. M. J.; Gilbert, A. T. B.; Gill, P. M. W. Communication: Hartree−Fock description of excited states of H_2. *J. Chem. Phys.* **2014**, *141*, 111104.
(12) Barca, G. M. J.; Gilbert, A. T. B.; Gill, P. M. W. Simple Models for Difficult Electronic Excitations. *J. Chem. Theory Comput.* **2018**, *14*, 1501−1509.
(13) Hait, D.; Head-Gordon, M. Excited State Orbital Optimization via Minimizing the Square of the Gradient: General Approach and Application to Singly and Doubly Excited States via Density Functional Theory. *J. Chem. Theory Comput.* **2020**, *16*, 1699−1710.
(14) Hait, D.; Head-Gordon, M. Orbital Optimized Density Functional Theory for Electronic Excited States. *J. Phys. Chem. Lett.* **2021**, *12*, 4517−4529.
(15) Carter-Fenk, K.; Herbert, J. M. State-Targeted Energy Projection: A Simple and Robust Approach to Orbital Relaxation of Non-Aufbau Self-Consistent Field Solutions. *J. Chem. Theory Comput.* **2020**, *16*, 5067−5082.
(16) Thom, A. J. W.; Head-Gordon, M. Locating Multiple Self-Consistent Field Solutions: An Approach Inspired by Metadynamics. *Phys. Rev. Lett.* **2008**, *101*, 193001.
(17) Jensen, K. T.; Benson, R. L.; Cardamone, S.; Thom, A. J. W. Modeling Electron Transfers Using Quasidiabatic Hartree−Fock States. *J. Chem. Theory Comput.* **2018**, *14*, 4629−4639.
(18) Burton, H. G. A.; Wales, D. J. Energy Landscapes for Electronic Structure. *J. Chem. Theory Comput.* **2021**, *17*, 151−169.
(19) Levi, G.; Ivanov, A. V.; Jónsson, H. Variational Density Functional Calculations of Excited States via Direct Optimization. *J. Chem. Theory Comput.* **2020**, *16*, 6968−6982.
(20) Levi, G.; Ivanov, A. V.; Jónsson, H. Variational calculations of excited states via direct optimization of the orbitals in DFT. *Faraday Discuss.* **2020**, *224*, 448−466.
(21) Hait, D.; Head-Gordon, M. Highly Accurate Prediction of Core Spectra of Molecules at Density Functional Theory Cost: Attaining Sub-electronvolt Error from a Restricted Open-Shell Kohn−Sham Approach. *J. Phys. Chem. Lett.* **2020**, *11*, 775−786.
(22) Schmerwitz, Y. L. A.; Ivanov, A. V.; Jónsson, E. Ö.; Jónsson, H.; Levi, G. Variational Density Functional Calculations of Excited States: Conical Intersection and Avoided Crossing in Ethylene Bond Twisting. *J. Phys. Chem. Lett.* **2022**, *13*, 3990−3999.
(23) Burton, H. G. A.; Gross, M.; Thom, A. J. W. Holomorphic Hartree−Fock Theory: The Nature of Two-Electron Problems. *J. Chem. Theory Comput.* **2018**, *14*, 607−618.
(24) Vaucher, A. C.; Reiher, M. Steering Orbital Optimization out of Local Minima and Saddle Points Toward Lower Energy. *J. Chem. Theory Comput.* **2017**, *13*, 1219−1228.
(25) Obermeyer, M.; Inhester, L.; Santra, R. Strategies for solving the excited-state self-consistent-field problem for highly excited and multiply ionized states. *Phys. Rev. A* **2021**, *104*, 023115.
(26) Shea, J. A. R.; Neuscamman, E. Communication: A mean field platform for excited state quantum chemistry. *J. Chem. Phys.* **2018**, *149*, 081101.
(27) Hardikar, T. S.; Neuscamman, E. A self-consistent field formulation of excited state mean field theory. *J. Chem. Phys.* **2020**, *153*, 164108.
(28) Tran, L. N.; Shea, J. A. R.; Neuscamman, E. Tracking Excited States in Wave Function Optimization Using Density Matrices and Variational Principles. *J. Chem. Theory Comput.* **2019**, *15*, 4790−4803.
(29) Tran, L. N.; Neuscamman, E. Improving Excited-State Potential Energy Surfaces via Optimal Orbital Shapes. *J. Phys. Chem. A* **2020**, *124*, 8273−8279.
(30) Hanscam, R.; Neuscamman, E. Applying generalized variational principles to excited-state-specific complete active space self-consistent-field theory. *J. Chem. Theory Comput.* **2022**, *18*, 6608−6621.
(31) Tran, L. N.; Neuscamman, E. Exploring Ligand-to-Metal Charge-Transfer States in the Photo-Ferrioxalate System Using Excited-State Specific Optimization. *J. Phys. Chem. Lett.* **2023**, *14*, 7454−7460.
(32) Marie, A.; Burton, H. G. A. Excited States, Symmetry Breaking, and Unphysical Solutions in State-Specific CASSCF Theory. *J. Phys. Chem. A* **2023**, *127*, 4538−4552.
(33) Feller, D.; Peterson, K. A.; Davidson, E. R. A systematic approach to vertically excited states of ethylene using configuration interaction and coupled cluster techniques. *J. Chem. Phys.* **2014**, *141*, 104302.
(34) Ryu, J.-S.; Hudson, B. S. A new interpretation of the electronic spectrum of ethylene from 6−8 eV. *Chem. Phys. Lett.* **1995**, *245*, 448−454.
(35) Huzinaga, S. Variational Calculation of Ethylene. *J. Chem. Phys.* **1962**, *36*, 453−457.
(36) Buenker, R. J.; Peyerimhoff, S. D.; Hsu, H. L. A new interpretation for the structure of the V − N bands of ethylene. *Chem. Phys. Lett.* **1971**, *11*, 65−70.
(37) Dunning, T. H.; Hunt, W. J.; Goddard, W. A. The theoretical description of the ($\pi\pi^*$) excited states of ethylene. *Chem. Phys. Lett.* **1969**, *4*, 147−150.
(38) Serrano-Andrés, L.; Merchán, M.; Nebot-Gil, I.; Lindh, R.; Roos, B. O. Towards an accurate molecular orbital theory for excited states: Ethene, butadiene, and hexatriene. *J. Chem. Phys.* **1993**, *98*, 3151−3162.
(39) Sunil, K. K.; Jordan, K. D.; Shepard, R. Application of the MC SCF method to the $\pi \rightarrow \pi^*$ excitation energies of ethylene. *Chem. Phys.* **1984**, *88*, 55−64.
(40) McMurchie, L. E.; Davidson, E. R. Configuration interaction calculations on the planar $^1(\pi, \pi^*)$ state of ethylene. *J. Chem. Phys.* **1977**, *66*, 2959−2971.
(41) Brooks, B. R.; Schaefer, H. F. N(1Ag), T(3B1u), and V(1B1u) states of vertical ethylene. *J. Chem. Phys.* **1978**, *68*, 4839−4847.
(42) Angeli, C. On the nature of the $\pi \rightarrow \pi^*$ ionic excited states: The V state of ethene as a prototype. *J. Comput. Chem.* **2009**, *30*, 1319−1333.
(43) Müller, T.; Dallos, M.; Lischka, H. The ethylene 1^1B_{1u} state revisisted. *J. Chem. Phys.* **1999**, *110*, 7176.
(44) Lindh, R.; Roos, B. O. A theoretical study of the diffuseness of the V($^1B_{1u}$) state of planar ethylene. *Int. J. Quantum Chem.* **1989**, *35*, 813−825.

https://doi.org/10.1021/acs.jctc.4c00212
J. Chem. Theory Comput. 2024, 20, 5105−5114

(45) Johnson, K. E.; Johnson, D. B.; Lipsky, S. The electron impact spectra of some mono-olefinic hydrocarbons. *J. Chem. Phys.* **1979**, *70*, 3844.
(46) Basch, H.; McKoy, V. Interpretation of Open-Shell SCF Calculations on the T and V States of Ethylene. *J. Chem. Phys.* **1970**, *53*, 1628−1637.
(47) Peyerimhoff, S. D.; Buenker, R. J. Vibrational analysis of the electronic spectrum of ethylene based on ab initio SCF-CI calculations. *Theor. Chim. Acta* **1972**, *27*, 243−264.
(48) Petrongolo, C.; Buenker, R. J.; Peyerimhoff, S. D. Nonadiabatic inverstigation of the V − N spectrum of ethylene in a new diabatic representation. *J. Chem. Phys.* **1983**, *78*, 7284−7289.
(49) Daday, C.; Smart, S.; Booth, G. H.; Alavi, A.; Filippi, C. Full configuration interaction excitations of ethene and butadiene: Resolution of an ancient question. *J. Chem. Theory Comput.* **2012**, *8*, 4441−4451.
(50) Ben-Nun, M.; Martínez, T. J. Ab initio molecular dynamics study of cis-trans photoisomerization in ethylene. *Chem. Phys. Lett.* **1998**, *298*, 57−65.
(51) Ben-Nun, M.; Martínez, T. J. Photodynamics of ethylene: ab initio studies of conical intersections. *Chem. Phys.* **2000**, *259*, 237−248.
(52) Barbatti, M.; Paier, J.; Lischka, H. Photochemistry of ethylene: A multireference configuration interaction investigation of the excited-state energy surfaces. *J. Chem. Phys.* **2004**, *121*, 11614−11624.
(53) Siegbahn, P. E. M.; Almlöf, J.; Heiberg, A.; Roos, B. O. The complete active space SCF (CASSCF) method in a Newton-Raphson formulation with application to the HNO molecule. *J. Chem. Phys.* **1981**, *74*, 2384−2396.
(54) Dalgaard, E. A quadratically convergent reference state optimization procedure. *Chem. Phys. Lett.* **1979**, *65*, 559−563.
(55) Dalgaard, E.; Jo/rgensen, P. Optimization of orbitals for multiconfigurational reference states. *J. Chem. Phys.* **1978**, *69*, 3833−3844.
(56) Yeager, D. L.; Jo/rgensen, P. Convergency studies of second and approximate second order multiconfigurational Hartree−Fock procedures. *J. Chem. Phys.* **1979**, *71*, 755−760.
(57) Helgaker, T.; Jørgensen, P.; Olsen, J. *Molecular Electronic-Structure Theory*; John Wiley & Sons, 2000.
(58) Das, G. Multiconfiguration self-consistent field (MCSCF) theory for excited states. *J. Chem. Phys.* **1973**, *58*, 5104−5110.
(59) Yeager, D. L.; Jørgensen, P. A numerical study of the convergency of second and approximate second-order multiconfiguration Hartree−Fock procedures. *Mol. Phys.* **1980**, *39*, 587−596.
(60) Yeager, D. L.; Albertsen, P.; Jo/rgensen, P. Mode damping in multiconfigurational Hartree−Fock procedures. *J. Chem. Phys.* **1980**, *73*, 2811−2816.
(61) Wales, D. J. Energy Landscapes: Applications to Clusters. In *Biomolecules and Glasses*; Cambridge University Press: Cambridge, 2004.
(62) Sun, Q.; Zhang, X.; Banerjee, S.; Bao, P.; Barbry, M.; Blunt, N. S.; Bogdanov, N. A.; Booth, G. H.; Chen, J.; Cui, Z. H.; et al. Recent developments in the PySCF program package. *J. Chem. Phys.* **2020**, *153*, 024109.
(63) Dunning, T. H. Gaussian basis sets for use in correlated molecular calculations. I. The atoms boron through neon and hydrogen. *J. Chem. Phys.* **1989**, *90*, 1007−1023.
(64) Kendall, R. A.; Dunning, T. H.; Harrison, R. J. Electron affinities of the first-row atoms revisited. Systematic basis sets and wave functions. *J. Chem. Phys.* **1992**, *96*, 6796−6806.
(65) Ditchfield, R.; Hehre, W. J.; Pople, J. A. Self-Consistent Molecular-Orbital Methods. IX. An Extended Gaussian-Type Basis for Molecular-Orbital Studies of Organic Molecules. *J. Chem. Phys.* **1971**, *54*, 724−728.
(66) Wolfram Research, Inc. *Mathematica*, Version 12.0.0: Champaign, IL, 2021. https://www.wolfram.com/mathematica (accessed May 17, 2024).
(67) Humphrey, W.; Dalke, A.; Schulten, K. VMD − Visual Molecular Dynamics. *J. Mol. Graphics* **1996**, *14*, 33−38.
(68) Loos, P.-F.; Scemama, A.; Blondel, A.; Garniron, Y.; Caffarel, M.; Jacquemin, D. A Mountaineering Strategy to Excited States: Highly Accurate Reference Energies and Benchmarks. *J. Chem. Theory Comput.* **2018**, *14*, 4360−4379.
(69) Gilmore, R. *Catastrophe Theory for Scientists and Engineers*, 1st ed.; Dover Publications Inc., 1993.
(70) Huynh, B. C.; Thom, A. J. W. Symmetry in Multiple Self-Consistent-Field Solutions of Transition-Metal Complexes. *J. Chem. Theory Comput.* **2020**, *16*, 904−930.
(71) Burton, H. G. A. Generalized nonorthogonal matrix elements: Unifying Wick's theorem and the Slater−Condon rules. *J. Chem. Phys.* **2021**, *154*, 144109.
(72) Burton, H. G. A. Generalized nonorthogonal matrix elements. II: Extension to arbitrary excitations. *J. Chem. Phys.* **2022**, *157*, 204109.
(73) Burton, H. G. A. LibGNME: A C++ library for evaluating non-orthogonal matrix elements in electronic structure. https://github.com/hgaburton/libgnme (accessed May 17, 2024).
(74) Loos, P.-F.; Boggio-Pasqua, M.; Scemama, A.; Caffarel, M.; Jacquemin, D. Reference Energies for Double Excitations. *J. Chem. Theory Comput.* **2019**, *15*, 1939−1956.
(75) Véril, M.; Scemama, A.; Caffarel, M.; Lipparini, F.; Boggio-Pasqua, M.; Jacquemin, D.; Loos, P.-F. QUESTDB: A database of highly accurate excitation energies for the electronic structure community. *Wiley Interdiscip. Rev.: Comput. Mol. Sci.* **2021**, *11*, No. e1517.
(76) Andersson, K.; Malmqvist, P.-Å.; Roos, B. O.; Sadlej, A. J.; Wolinski, K. Second-order perturbation theory with a CASSCF reference function. *J. Phys. Chem.* **1990**, *94*, 5483−5488.
(77) Andersson, K.; Malmqvist, P.-Å.; Roos, B. O. Second-order perturbation theory with a complete active space self-consistent field reference function. *J. Chem. Phys.* **1992**, *96*, 1218−1226.
(78) Angeli, C.; Cimiraglia, R.; Evangelisti, S.; Leininger, T.; Malrieu, J.-P. Introduction of n-electron valence states for multi-reference perturbation theory. *J. Chem. Phys.* **2001**, *114*, 10252−10264.
(79) Werner, H.-J.; Knowles, P. J. An efficient internally contracted multiconfiguration−reference configuration interaction method. *J. Chem. Phys.* **1988**, *89*, 5803−5814.
(80) Finley, J.; Malmqvist, P. Å.; Roos, B. O.; Serrano-Andrés, L. The multi-state CASPT2 method. *Chem. Phys. Lett.* **1998**, *288*, 299−306.

https://doi.org/10.1021/acs.jctc.4c00212
J. Chem. Theory Comput. 2024, 20, 5105−5114